RSC Advances

Surface Passivation of Titanium Dioxide via Electropolymerization Method to Improve the Performance of Dye-Sensitized Solar Cells

Journal:	*RSC Advances*
Manuscript ID	RA-ART-11-2015-025406.R1
Article Type:	Paper
Date Submitted by the Author:	17-Jan-2016
Complete List of Authors:	mazloum, mohammad; Yazd University, Department of Chemistry Khoshro, A.; Yazd Uni., Taghavinia, Nima; Sharif University of Technology, Physics Department Hosseinzadeh, Laleh; yazd university,
Subject area & keyword:	Energy research < Physical

Surface Passivation of Titanium Dioxide via Electropolymerization Method to Improve the Performance of Dye-Sensitized Solar Cells

Mohammad Mazloum-Ardakani [a,*], Alireza Khoshroo[a], Nima Taghavinia[b], Laleh Hosseinzadeh[a]

[a]Department of Chemistry, Faculty of Science, Yazd University, Yazd, 89195-741, I.R. Iran

[b] Physics Department, Sharif University of Technology, Tehran 14588, Islamic Republic of Iran

E-Mail: mazloum@yazduni.ac.ir

Phone No: 00983518211670

Fax No: 00983518210644

Mohammad Mazloum-Ardakani

E-Mail: mazloum@yazd.ac.ir

Phone No: 00983518211670

Fax No: 00983518210644

Alireza Khoshroo

E-Mail: khoshroo.a.r@gmail.com

Laleh Hosseinzadeh

E-Mail: l.hosseinzadeh2011@gmail.comm

Nima Taghavinia

E-Mail: taghavinia@sharif.edu

Surface Passivation of Titanium Dioxide via Electropolymerization Method to Improve the Performance of Dye-Sensitized Solar Cells

Mohammad Mazloum-Ardakani [a,*], Alireza Khoshroo[a], Nima Taghavinia[b], Laleh Hosseinzadeh[a]

[a]Department of Chemistry, Faculty of Science, Yazd University, Yazd, 89195-741, I.R. Iran
[b] Physics Department, Sharif University of Technology, Tehran 14588, Islamic Republic of Iran

Abstract

In dye-sensitized solar cells recombination reactions at the TiO_2 photoanode with electrolyte interface plays a critical role in the cell efficiency. Recombination of injected electrons in the TiO_2 with acceptors in the electrolyte usually occurs on uncovered area of TiO_2 surfaces. In this work, we report electropolymerization of polymer films on nanoporous TiO_2 electrode surfaces using an ionic liquid as the growth medium. The choice of ionic liquid as the growth medium for this study is based on the insolubility of dye N719 in this electrolyte, so avoiding dye molecules detachment from the TiO_2 photoanode surface over the entire potential range investigated during the electropolymerization. Consequently using this insulating and passivation polymer onto the open areas of a nanoporous TiO_2 surface the photovoltaic device efficiency most improved by 19%, furthermore, prevent detachment of dye molecules leads to an increase in stability of the dye-sensitized solar cells.

Keywords: Electropolymerization, Recombination, Dye-sensitized Solar Cells, Passivation, Titanium Dioxide

1. Introduction

Dye-sensitized solar cells (DSCs) have generated wide-spread attention in the about twenty years ago because of their low cost, relatively high efficiency and successful application future [1–3]. The efficiency of DSCs is determined by the open circuit voltage (V_{OC}), the short circuit current density (J_{SC}) and the fill factor (FF). In a typical DSC, a major hurdle for advancement of DSCs is the electron recombination at the TiO_2/electrolyte interface [4–6]. The interface between the TiO_2 photoanode and the electrolyte is important for the photovoltaic device efficiency. In respective photoelectrodes, the surfaces of the TiO_2 electrode are not quite coated with the dye molecules. Thus, electrons in a mesoporous TiO_2 film recombine with either oxidized species in electrolyte or oxidized sensitizer at the interfaces of TiO_2 film and with a conducting substrate resulting in the loss of photovoltaic performance of DSCs. Therefore, several methods have been attempted to restrain this process by introducing additives to electrolytes, such as guanidinium thiocyanate and 4-tert-butylpyridine [7–9], forming an extra thin layer onto TiO_2 [10–12], incorporation coadsorbents on the TiO_2 [13–15] and surface passivation by polymerization [16,17].

Polymer materials have unique properties which enable new applications in various fields [18–21]. Electrochemical synthesis of polymer is an excellent method to prepare polymer film on the surface of electrodes. In electropolymerization method, experimental parameters can control film thickness of polymer and charge transport characteristics. The electropolymerization is commonly performed by constant potential or constant current methods. Potential sweep methods such as CVs correspond to a repetitive triangular potential waveform applied on the electrode. The latter method has been mainly used to obtain qualitative information about the redox processes involved in the early stages of the polymerization reaction, and to examine the

electrochemical behavior of the polymer film after electrodeposition [22,23]. However applying electropolymerization on the TiO_2 electrode stained with the dye sensitizer causes dye desorption from the TiO_2 electrode in the aqueous or organic solvents. Therefore, a new strategy is needed that does not effect on the absorption of dye.

Ionic liquids (ILs) are by definition ionic melts with a melting point below 100 °C and widely employed as solvents for green organic and electrodeposition of polymer [24], which indicates that significant enhancements in selectivity, yield and reaction rate [25,26]. Ionic liquids with high ionic conductivities, catalytic properties, negligible vapor pressures and wide electrochemical windows have been obtained over a wide range of application [27–30]. These properties are very important for variety of electrochemical processes, and it has been shown that it is possible to be appropriate electrolyte for electropolymerization [31–33].

In this work, we developed a method to deposit a passivation layer of poly anthranilic acid (PAA) on the open areas of TiO_2 surface via electropolymerization in 1-Methyl-3-octylimidazolium hexafluorophosphate) [OMIM-PF_6]. The main object of this study was to introduce an electrochemical method for insulating and passivation open areas of a nanoporous TiO_2 in dye-sensitized solar cells. To the best of our knowledge, no study has been published so far reporting the surface passivation of N719-sensitized nanocrystalline TiO_2 electrode via electropolymerization method. It was found that the thin insulating PAA layer on TiO_2 surface decreased the electron recombination and thereby improved the photovoltaic device efficiency, as illustrated in Scheme 1. Furthermore, polymer passivation layers prevent desorption of N719 dye and improvements in the stability of the devices. Therefore, we investigated the effects and optimal conditions for electropolymerization of insulating PAA layer on the mesoporous TiO_2 surface on the photovoltaic performance of DSCs.

2. Experimental

2.1. Materials

The N719 dye and FTO glasses were purchased from Dyesol. 4-tert-butylpyridine, guanidinium thiocyanate, $TiCl_4$, H_2PtCl_6 and 1-Methyl-3-octylimidazolium hexafluorophosphate were reagent-grade from Sigma Aldrich. Acetonitrile, ethanol, solvents and reagents were of pro-analysis grade from Merck (Germany). The electrochemical experiments were performed by an Autolab potentiostat/galvanostat (PGSTAT-302 N, Eco Chemie, Netherlands). All potentials reported were versus the Ag/AgCl/KCl (3.0 M) electrode. Impedance measurements were performed with a potentiostat/galvanostat (IVIUM, Compactstat). The frequency range is 0.01-100 kHz, and the magnitude of the modulation signal is 10 mV. The spectra were measured with an external potential of −0.72 V in the dark.

Scanning electron microscopy (SEM) was used to examine the morphology of photoanode film (TESCAN SEM system). Infrared spectra were run on a Shimadzu model 8,300 Fourier Transform Infrared spectrophotometer. Ultraviolet–visible (UV–Vis) spectra were obtained by an Optizen 3220 UV UV–Vis spectrophotometer. The photovoltaic performances of the DSCs were measured under AM 1.5 simulated sunlight illumination (Luzchem-Solar) by a potentiostat/galvanostat (IVIUM, Compactstat).

2.2. Fabrication of DSCs devices

The platinized counter electrodes were prepared on a cleaned FTO-glass by ethanol solution of H_2PtCl_6 (2 mg of Pt in 1 mL of ethanol) followed by heating at 400◦C for 20 min [34]. The FTO glass plates were sequentially cleaned by ultrasound in 0.1 M HCl, acetone and ethanol (15 min for each step) and finally rinsed with distilled water. The TiO_2 paste was prepared by

hydrolysis of $TiCl_4$ according to previously reported methods[34]. A TiO_2 layer was fabricated on the FTO glass plates using doctor blade method and by sintering at 500 °C for 30 min. To sensitize the photoanode, when the TiO_2 layer was cooled to 80 °C, it was immersed in 0.3 mM N719 dye solution in a mixture of tert-butyl alcohol and acetonitrile (volume ratio, 1:1) and kept at room temperature for 18 h.

The electropolymerization of anthranilic acid was performed in a three-electrode electrochemical cell with TiO_2 electrode sensitized with N719 as working electrode, Ag wire and a platinum sheet as the counter electrode and the reference electrode, respectively. Before formation of polymer, the TiO_2 photoanode were immersed in the electrolyte for 5 min leaving the mesoporous film soaked fully. The synthesis of PAA layer was carried out by cyclic potential-scanning method between −0.2 and 1.2 V at 100 mV s^{-1}in OMIM-PF_6 containing 10.0 mM anthranilic acid (AA) at various cycle number (0-12 cycle). The amount of the deposit layers was controlled through the number of voltammetric scans. After the electropolymerization, the working electrode was taken out and rinsed vigorously with acetonitrile and chloroform to remove any soluble materials. The TiO_2 photoanode was then dried under vacuum for 30 min before further application.

N719 dye-containing photoelectrodes (electrode A) were employed for comparison of photovoltaic properties with the electrodes containing PAA (electrode B). The DSCs devices were assembled using a working (electrode A and B) and counter electrodes and onto a sandwich-type cell by heating with a 35 μm thick thermal adhesive film (Surlyn, Dyesol). Then a liquid electrolyte composed 0.6 M BMII, 0.03 M I_2, 0.5 M 4-tertbutylpyridine and 0.10 M guanidinium thiocyanate in a mixture of acetonitrile and valeronitrile (volume ratio, 85:15) were injected into the cells [35]. The organic solvent is a basic component in electrolytes; it gives an

environment for redox couple dissolution and diffusion. Generally, no single solvent can simultaneously fulfill all the requirements for ideal solvents in DSSCs. Therefore, for optimal DSCs performances, the mixed solvents are often used. A mixed solvent of acetonitrile and valeronitrile is considered as the best electrolyte [2]. The redox couple is a key component of the DSSCs. The iodide/triiodide has been demonstrated as the most efficient redox couple for regeneration of the oxidized dye. When BMII incorporated into electrolyte, IL can be both the source of iodide and the solvent itself. Additives are another component in electrolyte. 4-tertbutylpyridine and guanidinium thiocyanate could enhance V_{oc} and electron lifetime, respectively [3].

Insert Scheme 1

3. Results and discussion

3.1. Electropolymerization and Materials Characterization

Figure 1A represents cyclic voltammograms in the course of polymerization of AA at 9 times of potential scanning in OMIM-PF_6. As can be seen, the first cycle of the electropolymerization of AA shows one anodic peak (E_p = 0.38 V), which correspond to the oxidation of AA to its radical cation and its cathodic peak near 0.21 V. In the second cycle, indicating the occurrence of an oxidation peak at 0.41 V, and cathodic peak at 0.23 V. These peaks may be related to the transformation from quinoid structure to aromatic state. A mechanism of copolymerization of PAA is proposed in Figure 1S. As shown in figure 1, with increasing the potential scanning cycle, the anodic and cathodic peak currents increased. This is indicative that the thickness of the insulating PAA layer on the mesoporous TiO_2 surface increased. Furthermore, the potential of oxidation peak was shifted to negative potentials due to

the increase of the charge transfer resistance in the PAA layer and the over-potential is needed to overcome the resistance [36].

In order to obtain more details on the electropolymerization of AA, cyclic voltammograms of TiO_2 electrode and TiO_2 electrode stained with the N719 was performed in the absence (curve a, c in Fig. 1B) and the presence of AA (curve b, d in Fig. 1B). Cyclic voltammetry of TiO_2 electrode with N719 adsorbed exhibits one anodic and the corresponding cathodic peak, which correspond to the conversion of Ru (II) to Ru (III) and vice versa within a quasi-reversible one-electron process (curve c, figure 1B) [37]. At the first cycle of electropolymerization (curve d, figure 1B), there is broader oxidation peaks with current onset at about 0.38 V, which is corresponding to the oxidation of the N719 on nanoporous TiO_2 surface and monomer AA to its cation radical.

Insert Figure 1

Figure 2S shows the FT-IR spectrum of PAA, TiO_2 and PAA on TiO_2 between 500 and 4000 cm^{-1}. The peaks at 3418, 2920, 1693, 1603, 1510, 1498, 1451, 1348, 1249, and 1070 cm^{-1} generally appear in the FT-IR spectrum of PAA. These peaks are in good agreement with the literature data [38]. Therefore, the bands were almost similar to PAA indicating the absence of any kind of chemical interaction between the PAA and the photoanode.

The effect of electropolymerization process on the amount of dye loading on TiO_2 was investigated by ultraviolet–visible spectroscopy (Fig. 2). It is clear the dye adsorption of electrode B showed similar amount of dye with that of the bare TiO_2 (without electropolymerization). These results suggest that the electropolymerization process did not

effect on the amount of N719 adsorbed to DSCs with N719 dye alone (electrode A) and with PAA (electrode B). The similar shape of the absorption spectra before and after the electropolymerization have been shown the N719 molecules do not participate on the electrochemical polymerization of PAA. Therefore, electropolymerization process of PAA on the TiO_2 electrode surface does not have any influence on the molecular structure of the N719 dye.

Insert Figure 2

In the following, in order to investigate characteristics of OMIM-PF_6 as a electrolyte, the electropolymerization was also carried out in conventional electrolyte such as acetonitrile solutions as shown in figure 3S and its effect on the optical absorption of dye was compared with that in OMIM-PF_6 (see figure 4S). As can be seen, the main absorption band at 530 nm is observed in all three spectra. The electropolymerization of the electrode B in OMIM-PF_6 does not lead to a significant change in color, and indeed the UV/Vis spectrum of the sample after electropolymerization still shows a strong band for the N719. But the electropolymerization in acetonitrile, new weaker absorption bands appear at 440 nm and 660 nm. Desorption of the N719 dye into 0.1 M KOH followed by UV/Vis analysis confirms that 29% of the dye molecules is detachment from the TiO_2 photoanode surface or converted.

TEM was used to study the topography of TiO_2 electrodes before and after electropolymerization (Fig 3a-d). Figure 3a, b show TEM images of TiO_2 nanoparticles covered with PAA films. The polymer film (PAA) grew on the surface of TiO_2 particles by about 1 nm thickness, demonstrating that the PAA formed via electropolymerization on the surfaces of the nanocrystalline TiO_2 particles. SEM images of electrode B and electrode A also clearly demonstrated polymer film growth (Figure 5S, Supporting Information).

Insert Figure 3

After electropolymerization on the mesoporous TiO_2 film, PAA has covered within the pores of a TiO_2 film and compact PAA layers have been formed on the TiO_2 electrode surface prevented the electrolyte from a direct contact with the TiO_2 surface. Furthermore, the PAA film does not significantly affect the mesoporous structure of the TiO_2 photoanode. These results demonstrated that the electropolymerization produced the polymer film encapsulating TiO_2 nanoparticles.

3.2. Photovoltaic Performance

The influence of the polymer films on nanoporous TiO_2 electrode surfaces on photovoltaic performance was measured under AM 1.5 solar conditions. PAA can be promptly deposited on TiO_2 through electropolymerization, and its thickness can be well controlled by cycle number. DSCs with PAA film at various cycle numbers were fabricated and characterized (Figure 4 A; and figure 6S, Supporting Information). In device A, TiO_2 photoanode sensitized with the N719 dye alone give rise to photovoltaic device efficiency (η) of 6.38 % (Jsc＝14.20 mA cm^{-2}, V_{OC}＝744 mV), as shown in figure 4B. The photovoltaic device performance of DSCs is sensitive to the cycle number of the electropolymerization. The V_{OC} and J_{SC} values increase after three, six and nine cycles of electropolymerization (Figure 4 A), showing an optimum efficiency of 7.6% after nine cycles. It is noteworthy that in the presence of PAA [9 cycles], J_{SC} and V_{OC} yielded a 10.5% and 4.7% improvement, respectively. Both the V_{OC} and J_{SC} values decrease with the further increase in the cycle number of the polymerization. The decrease in

efficiency with increasing PAA thickness may be due to the decreased electron injection yield as reported in the literature [39]. The dark current (Inset of figure 4B) decreases with deposit a passivation layer of PAA, indicating that the recombination between electrons in TiO_2 photoanode and tri-iodide ions being retarded by the polymer film (recombination reaction in Scheme 1), which may be attributed to the blocking effect of insulating film on the TiO_2 surface. The increase in V_{OC} and J_{SC} after electropolymerization of PAA can be attributed to this decrease in recombination rate.

Insert Figure 4

In order to further understanding of the role of the deposit a passivation layer of PAA on the higher V_{OC}, EIS were used to gain data about the interfacial electron transfer processes. The EIS Nyquist plot, shown in figure 5, exhibits two arcs or semicircles for the charge transfer resistance at the counter electrode/electrolyte interface at high frequency and TiO_2 electrode/electrolyte interface at lower frequencies [40].

Insert Figure 5

R_{ct} was estimated to be 74 Ω for the DSCs with bare TiO_2 electrode (device A) and 153 Ω for DSCs with deposit a passivation layer of PAA on TiO_2 electrode, meaning electron recombination resistance increased in the presence of PAA layer on TiO_2 photoanode, thus resulting in higher V_{OC}. Thus, the insulating PAA layer on TiO_2 electrode can reduce the charge recombination. Consequently, the electron recombination in DSCs without PAA is faster than that forms an insulating film of PAA on the TiO_2 surface. Electron lifetime (τ), as remarkable

parameter to estimate the electron recombination rate, is usually derived by R_{rec} and Cμ ($\tau = R_{ct} * C\mu$) from EIS [41]. The insulating film of PAA on the TiO_2 surface also increased the electron lifetime from 35.2 ms to 79.3 ms. This increase electron lifetime is accompanied with an increasing in the electron transfer resistance, indicating that the PAA film decreases the electron capture by electron acceptors in electrolyte. The increased electron lifetime mainly accounts for the increased V_{OC}. Therefore, this property can be attributed to that the PAA layer of yields insulating layer between the conduction band electrons and triiodide ions in the electrolyte, which could reduce the recombination of electrons in TiO_2 film with acceptor species in the electrolyte.

To investigate the role of the PAA layer on the changes in the surface trapping sites and to reveal the change in V_{OC}, CVs experiments were carried out on electrode A and B (Figure 6A). Higher density of trap states at the surface of mesoporous TiO_2 film may induce higher recombination rate of electrons and lower V_{OC}. The cyclic voltammograms can be affected by the presence of coordinatively unsaturated Ti species on the surface of TiO_2 [42].

Insert Figure 6

The capacitive currents of the TiO_2 electrode (electrode A) and TiO_2 coated with PAA layer (electrode B) displayed gradual onsets under a forward bias (Figure 6B) [4]. The current increases much more slowly for the TiO_2 coated with PAA layer (electrode B) than that for the TiO_2 electrode (electrode A) in CVs. The onset is about -0.78 V for electrode sensitized with N719 dye alone, whereas in the presence of the PAA layer on the TiO_2, it moves to -0.82 V, indicating that the edge of conduction band of TiO_2 moved negatively toward the vacuum level.

This shift is due to insulating PAA layer on TiO_2 surface. Moreover, the slope (dQ/dV) of TiO_2 electrode was large, and the slope decreased after electropolymerization of PAA (TiO_2 coated with PAA layer).

These results indicate that coverage of the TiO_2 by PAA layer can reduce the density of surface trap states. The surface of the TiO_2 electrode is not quite coated with the dye molecules; therefore, there are some uncovered areas of directly in contact with the electrolyte. In the presence of PAA as insulating film covered these surface areas, resulting in a decrease in trap states.

The photovoltaic performances (J_{SC}, V_{OC} and η) of the devices were measured under thermal aging experiments at 60 °C in the dark conditions to measure the effect of the polymer layer covering the TiO_2 nanoparticles on the long-term stability (Figure 7S, Supporting Information). After 600 h, η and J_{SC} of electrode A dropped by more than 34% and 31%, respectively. During the whole aging process, a relatively small extent in V_{OC} was noted. This poor stability is due to detachment of N719 dye molecules from the surfaces of TiO_2 photoanode. On the other hand, electrode B, which included an polymer layer covering the TiO_2 particles, showed excellent stability, remaining over 94% of its initial η. The decrease in J_{SC} was 8%, which indicated that the stability of N719 molecules on the electrode B due to the presence of the PAA layers on TiO_2 electrode. This film insulates the N719 and decreased detachment of N719 molecules from the surface of the mesoporous TiO_2 electrode (Figure 8S, Supporting Information).

4. Conclusions

In summary, we successfully deposit a passivation layer of PAA on TiO_2 nanoparticles surface using electropolymerization of the AA. A polymer film can remarkably improve the photovoltaic device performance of DSCs. The photovoltaic device performance is dependent to the thickness of the PAA, which can control through the number of voltammetric scans. These findings open the way for using an electropolymerization as a coating method in DSCs. The choice of ionic liquid as the growth medium is based on the insolubility of dye in this electrolyte, so avoiding dye molecules detachment from the TiO_2 photoanode surface over the entire potential range investigated during the electropolymerization. This method can be used for other dye molecules which insoluble in this electrolyte. The polymer film effect on the photovoltaic device performance of DSCs due to the passivation of the TiO_2 surface, negatively shift of the conduction band of TiO_2, decreases of the electron combination and retardation of detachment of N719 molecules from the surfaces of mesoporous TiO_2 photoanode.

ACKNOWLEDGMENT

The authors wish to thank the Yazd University Research Council, IUT Research Council and Excellence in Sensors for financial support of this research.

References

1. N. Sharifi, F. Tajabadi, and N. Taghavinia, *ChemPhysChem*, 2014, **15**, 3902–3927.

2. J. Wu, Z. Lan, J. Lin, M. Huang, Y. Huang, L. Fan, and G. Luo, *Chem. Rev.*, 2015, **115**, 2136–2173.

3. A. Hagfeldt, G. Boschloo, L. Sun, L. Kloo, and H. Pettersson, *Chem. Rev.*, 2010, **110**, 6595–6663.

4. J. Lim, Y. S. Kwon, and T. Park, *Chem. Commun.*, 2011, **47**, 4147–4149.

5. F. Fabregat-Santiago, J. García-Cañadas, E. Palomares, J. N. Clifford, S. A. Haque, J. R. Durrant, G. Garcia-Belmonte, and J. Bisquert, *J. Appl. Phys.*, 2004, **96**, 6903–6907.

6. D.-L. Gao, Y. Wang, P. Zhang, L.-M. Fu, X.-C. Ai, and J.-P. Zhang, *RSC Adv.*, 2015, **5**, 84959–84966.

7. Z. Zhang, N. Evans, S. M. Zakeeruddin, R. Humphry-Baker, and M. Grätzel, *J. Phys. Chem. C*, 2007, **111**, 398–403.

8. C. Zhang, Y. Huang, Z. Huo, S. Chen, and S. Dai, *J. Phys. Chem. C*, 2009, **113**, 21779–21783.

9. T. M. Koh, K. Nonomura, N. Mathews, A. Hagfeldt, M. Gratzel, S. G. Mhaisalkar, and A. C. Grimsdale, *J. Phys. Chem. C*, 2013, **117**, 15515–15522.

10. Y. Diamant, S. G. Chen, O. Melamed, and A. Zaban, *J. Phys. Chem. B*, 2003, **107**, 1977–1981.

11. H.-J. Son, X. Wang, C. Prasittichai, N. C. Jeong, T. Aaltonen, R. G. Gordon, and J. T. Hupp, *J. Am. Chem. Soc.*, 2012, **134**, 9537–9540.

12. H. Yu, B. Xue, P. Liu, J. Qiu, W. Wen, S. Zhang, and H. Zhao, *ACS Appl. Mater. Interfaces*, 2012, **4**, 1289–1294.

13. R. Hou, S. Yuan, X. Ren, Y. Zhao, Z. Wang, M. Zhang, D. Li, and L. Shi, *Electrochim. Acta*, 2015, **154**, 190–196.

14. M. Mazloum-Ardakani and A. Khoshroo, *Phys. Chem. Chem. Phys.*, 2015, **17**, 22985–22990.

15. Y.-G. Lee, D. Song, J. H. Jung, S. Wooh, S. Park, W. Cho, W. Wei, K. Char, and Y. S. Kang, *RSC Adv.*, 2015, **5**, 68413–68419.

16. S. M. Feldt, U. B. Cappel, E. M. J. Johansson, G. Boschloo, and A. Hagfeldt, *J. Phys. Chem. C*, 2010, **114**, 10551–10558.

17. S. Park, J. Lim, I. Y. Song, N. Atmakuri, S. Song, Y. S. Kwon, J. M. Choi, and T. Park, *Adv. Energy Mater.*, 2012, **2**, 219–224.

18. D. R. Paul and L. M. Robeson, *Polymer (Guildf).*, 2008, **49**, 3187–3204.

19. M. Mazloum-Ardakani, M. A. Sheikh-Mohseni, and A. Benvidi, *Electroanalysis*, 2011, **23**, 2822–2831.

20. K. Miyatake, Y. Chikashige, E. Higuchi, and M. Watanabe, *J. Am. Chem. Soc.*, 2007, **129**, 3879–3887.

21. J. Mindemark, B. Sun, E. Törmä, and D. Brandell, *J. Power Sources*, 2015, **298**, 166–170.

22. S. Sadki, P. Schottland, N. Brodie, and G. Sabouraud, *Chem. Soc. Rev.*, 2000, **29**, 283–293.

23. M. Mazloum-Ardakani, A. Khoshroo, D. Nematollahi, and B.-F. Mirjalili, *J. Electrochem. Soc.*, 2012, **159** , H912–H917.

24. M. Armand, F. Endres, D. R. MacFarlane, H. Ohno, and B. Scrosati, *Nat. Mater.*, 2009, **8**, 621–629.

25. M. Mazloum-Ardakani, A. Khoshroo, and L. Hosseinzadeh, *Sensor. Actuator. B. Chem.*, 2014, **204**, 282–288.

26. M. Mazloum-Ardakani and A. Khoshroo, *Electrochim. Acta*, 2014, **130**, 634–641.

27. M. Barghamadi, A. S. Best, A. I. Bhatt, A. F. Hollenkamp, P. J. Mahon, M. Musameh, and T. Rüther, *J. Power Sources*, 2015, **295**, 212–220.

28. X. Kang, J. Zhang, W. Shang, T. Wu, P. Zhang, B. Han, Z. Wu, G. Mo, and X. Xing, *J. Am. Chem. Soc.*, 2014, **136**, 3768–3771.

29. M. Mazloum-Ardakani and A. Khoshroo, *Electrochem. commun.*, 2014, **42**, 9–12.

30. M. Mazloum-Ardakani, L. Hosseinzadeh, and A. Khoshroo, *J. Electroanal. Chem.*, 2015, **757**, 58–64.

31. R. D. Rogers and K. R. Seddon, *Science*, 2003, **302**, 792–793.

32. K. R. Seddon, *Nat. Mater.*, 2003, **2**, 363–365.

33. J. F. Stanzione, R. E. Jensen, P. J. Costanzo, and G. R. Palmese, *ACS Appl. Mater. Interfaces*, 2012, **4**, 6142–6150.

34. S. Ito, T. N. Murakami, P. Comte, P. Liska, C. Grätzel, M. K. Nazeeruddin, and M. Grätzel, *Thin Solid Films*, 2008, **516**, 4613–4619.

35. L. Giribabu, T. Bessho, M. Srinivasu, C. Vijaykumar, Y. Soujanya, V. G. Reddy, P. Y. Reddy, J.-H. Yum, M. Grätzel, and M. K. Nazeeruddin, *Dalt. Trans.*, 2011, **40**, 4497–4504.

36. S. Cosnier and A. Karyakin, *Electropolymerization: concepts, materials and applications*, John Wiley & Sons, 2010.

37. A. J. Bard and L. R. Faulkner, *Electrochemical Methods: Fundamentals and Applications*, Wiley, 2nd edn., 2000.

38. Y. Wang and W. Knoll, *Anal. Chim. Acta*, 2006, **558**, 150–157.

39. E. Palomares, J. N. Clifford, S. A. Haque, T. Lutz, and J. R. Durrant, *J. Am. Chem. Soc.*, 2003, **125**, 475–482.

40. Q. Wang, J.-E. Moser, and M. Grätzel, *J. Phys. Chem. B*, 2005, **109**, 14945–14953.

41. J. Bisquert, F. Fabregat-Santiago, I. Mora-Seró, G. Garcia-Belmonte, and S. Giménez, *J. Phys. Chem. C*, 2009, **113**, 17278–17290.

42. Z. Zhang, S. M. Zakeeruddin, B. C. O'Regan, R. Humphry-Baker, and M. Grätzel, *J. Phys. Chem. B*, 2005, **109**, 21818–21824.

Legends for the Figures and Table:

Scheme 1 Schematic representation of the charge-transfer processes in the presence of PAA insulting layer at the mesoporous TiO_2 film /electrolyte interface of DSCs. well as show the effects of PAA insulting layer on the electron recombination and V_{OC}.

Figure 1 (A) CVs recorded during the polymerization of 10.0 mM AA at 9 times of potential scanning in OMIM -PF_6, (B) CVs of TiO_2 electrode (a) and N719/ TiO_2 electrode (c) in OMIM PF_6, (b) as (a) + 10.0 mM AA and (d) as (c) + 10.0 mM AA.

Figure 2 The UV-Vis spectra of the N719 dye from the TiO_2 photoanode without (electrode A) and with PAA layer coated (electrode B).

Figure 3 TEM photographs of TiO_2 particles encapsulated with polymer film (a and b) and bare TiO_2 particles (c and d).

Figure 4 (A) Detailed cycle number evolution of photovoltaic parameters of electrode B. (B) The I-V results of the electrode sensitized with N719 dye alone (device A) and with PAA film (device B [9 cycle]), Inset: In the dark condition.

Figure 5 The EIS Nyquist plot of the device with N719 alone (device A) and with PAA film (device B) under the dark condition.

Figure 6 (A) CVs of TiO_2 (electrode A) and TiO_2 coated with PAA layer (electrode B) the scan rate is 0.05 Vs^{-1}. (B) Energy levels at the photoanode/ electrolyte interface.

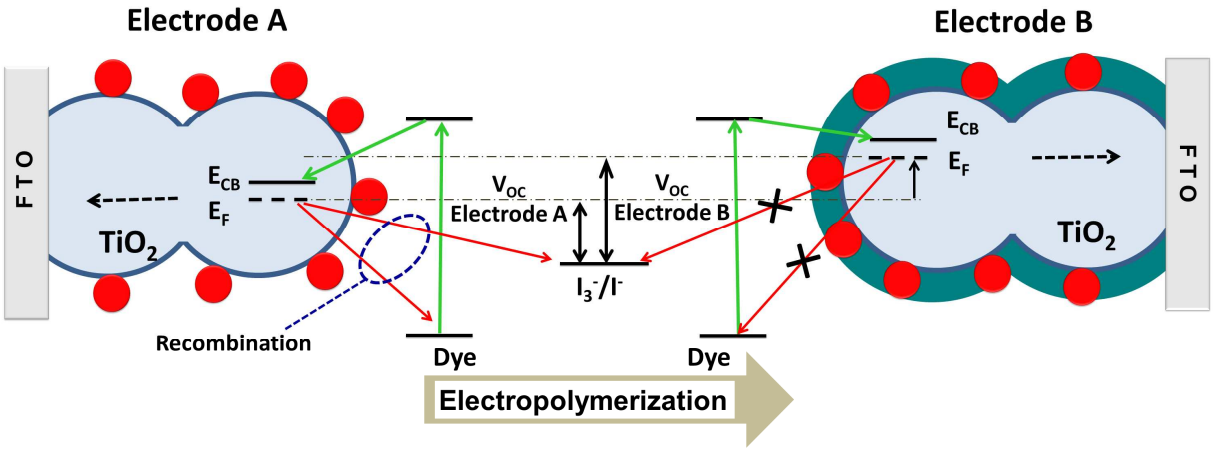
Electrode A
Electrode B
FTO
FTO
E_{CB}
E_F
TiO_2
E_{CB}
E_F
TiO_2
V_{OC}
Electrode A
V_{OC}
Electrode B
I_3^-/I^-
Recombination
Dye
Dye
Electropolymerization

Scheme 1

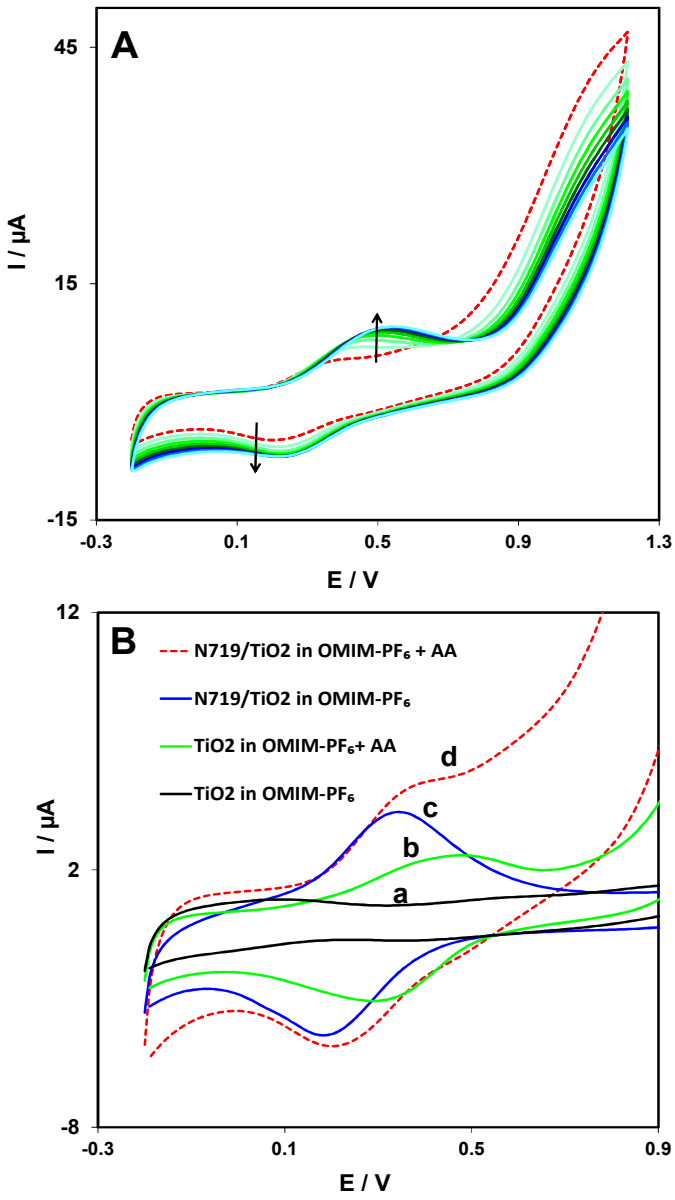
A
45
15
-15
I / μA
-0.3
0.1
0.5
0.9
1.3
E / V
B
12
2
-8
I / μA
N719/TiO2 in OMIM-PF6 + AA
N719/TiO2 in OMIM-PF6
TiO2 in OMIM-PF6+ AA
TiO2 in OMIM-PF6
d
c
b
a
-0.3
0.1
0.5
0.9
E / V

Figure 1

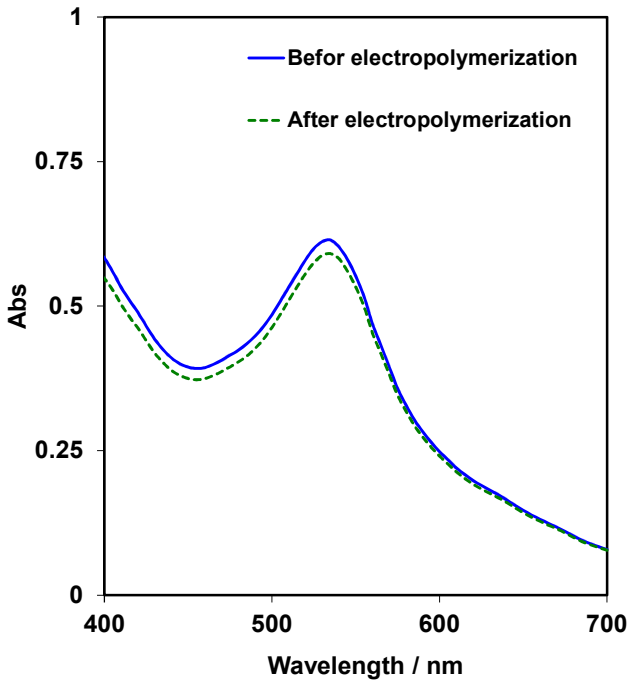
Befor electropolymerization
After electropolymerization
Abs
1
0.75
0.5
0.25
0
400
500
600
700
Wavelength / nm

Figure 2

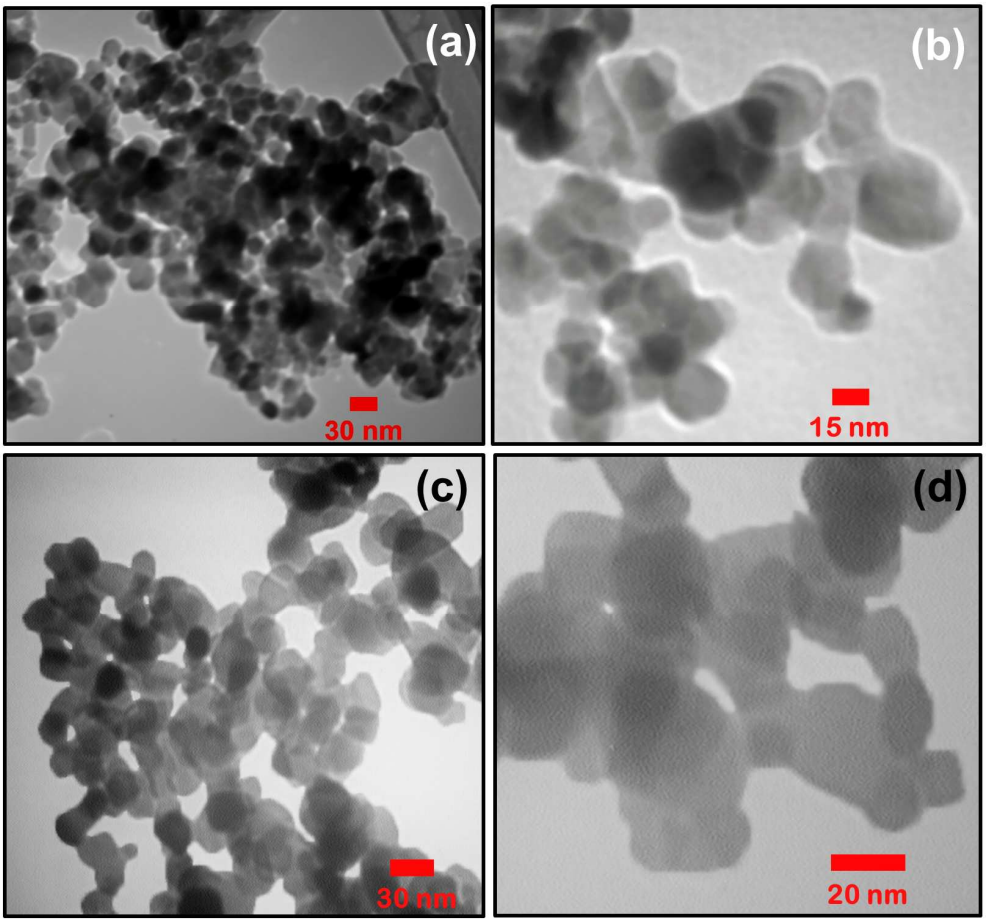

Figure 3

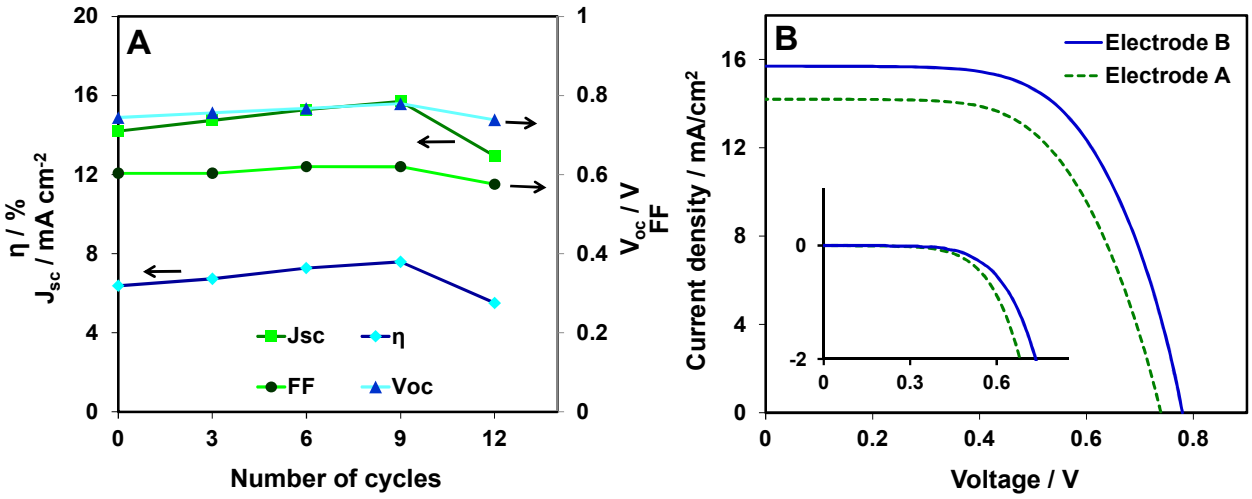
A
η / %
J_{sc} / mA cm^{-2}
V_{oc} / V
FF
Jsc
η
FF
Voc
Number of cycles
B
Electrode B
Electrode A
Current density / mA/cm^2
Voltage / V

Figure 4

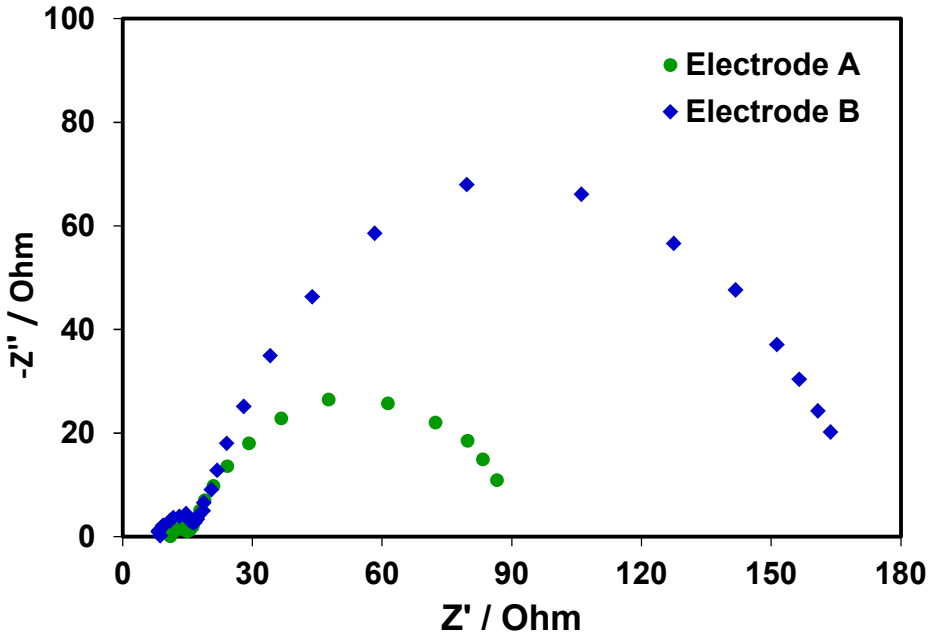
Electrode A
Electrode B
-Z'' / Ohm
Z' / Ohm
0
20
40
60
80
100
0
30
60
90
120
150
180

Figure 5

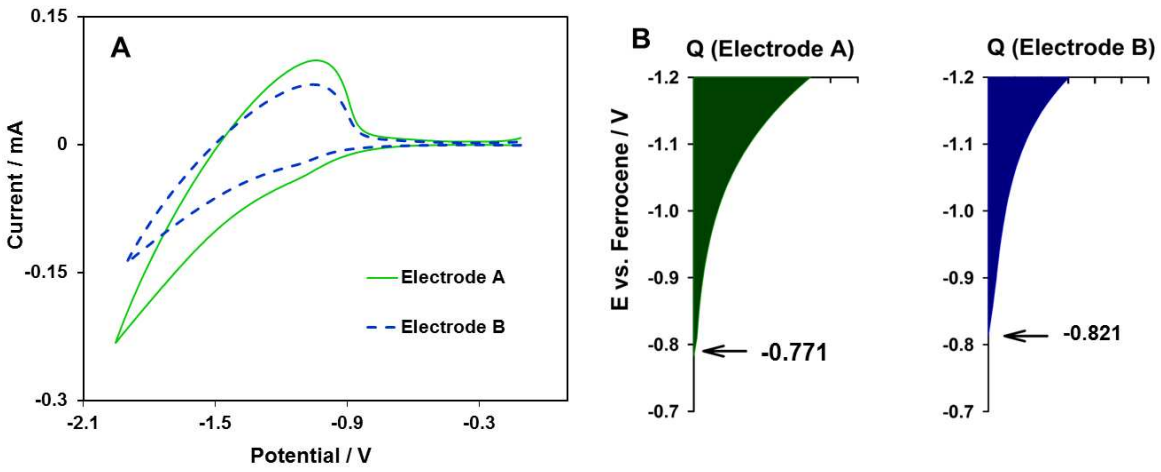
A
Current / mA
0.15
0
-0.15
-0.3
-2.1
-1.5
-0.9
-0.3
Potential / V
Electrode A
Electrode B
B
Q (Electrode A)
E vs. Ferrocene / V
-1.2
-1.1
-1.0
-0.9
-0.8
-0.7
-0.771
Q (Electrode B)
-0.821

Figure 6

Graphical abstract

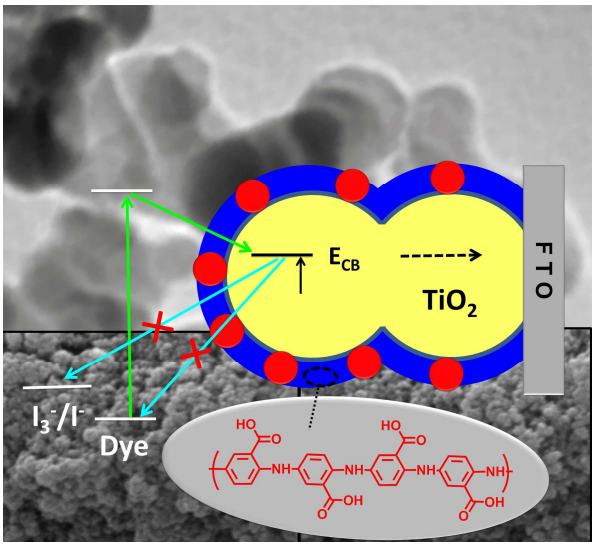

We introduce an electrochemical method for insulating and passivation open areas of a nanoporous TiO_2 in dye-sensitized solar cells, which can effectively decrease the recombination rate of electrons.